Birefringence and optical activity of [N(CH₃)₄]₂ZnCl₄

E Dijkstra, M Kremers and H Meekes

Research Institute for Materials, Faculty of Science, University of Nijmegen, Toernooiveld, 6525 ED Nijmegen, The Netherlands

Abstract. The birefringence and optical activity of [N(CH₃)₄]₂ZnCl₄ in phases I, II, III and IV have been measured with a high-accuracy universal polarimeter for six samples, all with different orientations. The birefringences clearly show the phase transitions. From the data, the diagonal components g_{ii} of the second-rank gyration pseudotensor could be determined and the off-diagonal components g_{ij} can be estimated. The results can be interpreted with the mesoscopic description of Dijkstra, Janner and Meekes which is especially applicable to the incommensurately modulated phase (II), but also to the multidomain monoclinic phase (IV).

1. Introduction

The discoveries of an incommensurately modulated phase in Na_2CO_3 by de Wolff in 1972 and in K_2SeO_4 by Iizumi et al in 1977 triggered the interest in materials with this new type of phase. Since then, a large number of insulators with an incommensurate (INC) phase have been investigated. A major part of this work has been dedicated to the A_2BX_4 family of dielectrics with an INC phase (see e.g. Hogervorst 1986). Many different physical properties have been measured (see Cummins 1990). In 1981 Kobayashi et al and in 1985 Uesu and Kobayashi reported the presence of optical activity in the INC phase of $(NH_4)_2BeF_4$ and in 1985 this phenomenon was also reported for other members of the A_2BX_4 group (Uesu and Kobayashi 1985). Until that moment the point group of the average structure of the INC phase was expected to describe the relevant symmetry for the optical properties. The investigated materials have centrosymmetric point groups for their paraphase and on the average for their INC phase and therefore no optical activity should be found. Kobayashi et al (1981) investigated only the g_{13}-component (notation in the setting of table 1 in the next section) of the gyration tensor. This component is the only one that becomes non-zero in the lock-in phase (the phase below the INC phase for which the modulation wave becomes commensurate). There remains the question whether the observed gyration in the INC phase is merely a precursor effect for the lock-in phase or explicitly due to the incommensurate nature of the modulation. For a more thorough investigation of this phenomenon it is important to determine all the coefficients g_{ij} of the axial second rank gyration tensor. Meekes and Janner (1988) did that for three components in the case of Rb_2ZnBr_4. In the INC phase g_{13} is unequal to zero and g_{11} and g_{12} are zero within the experimental error. This can be understood only partly by the fact that in the lower temperature region in the INC phase the structure of the lock-in phase (this is the phase below the INC phase for which the INC modulation with

wavevector $q = \gamma c^*$ becomes commensurate: $\gamma = 1/3$) is already manifest. The lock-in phase is non-centrosymmetric (space group $Pc2_1n$) and has a non-zero g_{13}. But the problem is that this cannot explain why g_{13} is unequal to zero in the whole INC phase.

Table 1. The phases occurring in TMAZC. The phase transition temperatures, the modulation wavevector ($q = \gamma c^*$) and the space groups are given.

Phase	VI	V	IV	III	II	I
T (K)	< 161	< 181	< 276.5	< 280	< 297.6	> 297.6
γ	1/3	0	1/3	2/5	inc.	0
Symmetry	$P2_12_12_1$	$P2_1/c11$	$P112_1/n$	$Pc2_1n$	$Pcmn(00\gamma)(1s\bar{1})$	$Pcmn$

Meekes and Janner (1988) showed that in the INC phase there can be a place-dependent gyration tensor that varies periodically along the direction of the modulation wave (i.e. c). How this can give rise to a macroscopic optical activity is described by Dijkstra (1991) and Dijkstra *et al* (1992). But to verify these theories more data has to be obtained for different materials and for more components of the gyration tensor.

In this paper we will present the optical activity and birefringence of $[N(CH_3)_4]_2ZnCl_4$ (tetramethylammonium tetrachlorozincate, in short TMAZC) obtained for six different directions. From these data we can derive the behaviour with temperature of all the components Δn_{ij} of the birefringence and of the diagonal components g_{ii} of the optical activity. It is not possible to extract the off-diagonal components of the optical activity from the data (as will be explained in section 6), but some conclusions for the behaviour of these with temperature can be given.

The data were obtained with a high-accuracy universal polarimeter (HAUP). For a description of the principles and design of this type of polarimeter see Kobayashi and Uesu (1983), Kobayashi *et al* (1986), Moxon and Renshaw (1990), and Dijkstra *et al* (1991). In this paper we will show that the fitting procedure of Moxon and Renshaw to obtain from the HAUP data the optical properties can give slightly different results than that of Kobayashi *et al* (1986). The latter assume the optical activity to be zero in the high temperature phase (the phase above the INC phase). They need this assumption in order to be able to interpret their data. Although this can give rise to a slightly different result, the conclusion that the INC phase is optically active remains. Moxon and Renshaw derived that by measuring along different extinction directions one circumvents these problems, because this gives additional information. An important support for the approach of Moxon and Renshaw is the fact that we find for measurements with different samples that this fitting procedure gives the ellipticities of the polarizers independent of the different orientations of the different samples. Furthermore, we find that also in the high-temperature phase of TMAZC there is optical activity present, revealing precursive effects of the INC phase.

2. The phases of TMAZC

In table 1 the different structural phases of TMAZC are listed together with the space groups that describe the symmetry of that phase. Phase II is the INC phase where the

modulation wavevector $q = \gamma c^*$ varies with temperature: $\gamma \approx 0.420$ just below T_i $= 297.6$ K, the transition temperature between the high-temperature phase I and the INC phase, to $\gamma \approx 0.408$ just above the lock-in temperature $T_c = 280$ K at which γ jumps to the commensurate value 2/5 (Madariaga *et al* 1987). The symmetry of the INC phase can be described by the superspace group $Pcmn(00\gamma)(1s\bar{1})$ (Madariaga *et al* 1987). At $T_m = 276.5$ K the orthorhombic lock-in phase (III) goes over into a monoclinic phase. Below that phase there are two more different phases, which we will not discuss here.

3. The samples

The TMAZC crystals were grown from aqueous solutions by the method of Arend *et al* (1986), which is based on thermally induced convection of the solution. The obtained crystals were oriented on the basis of their morphology and were then sawed and polished. We used an accurate and stable specimen holder and polished consecutively with silicon carbide papers 800 and 4000 and diamond pastes 45 μm, 25 μm and 2.5 μm. Thus we obtained good optical quality samples with reflecting, plane-parallel surfaces. Regarding the flatness needed to allow for a well defined retardation, we can make the following estimation. Suppose a sample is not plane-parallel and has a thickness that varies from d to $d + \delta d$, then the retardation Δ changes over its surface by an amount of

$$\delta\Delta = \frac{2\pi}{\lambda}\delta d\Delta n \tag{1}$$

where λ is the wavelength of the incident light and Δn is the birefringence. For materials with a too large birefringence it can be difficult to prepare samples for which $\delta\Delta$ is smaller than π. Then it is impossible to determine the retardation at all. For TMAZC this is not a problem because, as we will see in the next section, its birefringences are very small (in the order of 10^{-4} or less). With an accuracy of $\delta d = 2$ μm or better (the plane-parallelity of the samples after polishing) we have $\delta\Delta < 0.002$ rad.

The samples were adhered with thermo paste at the cold finger in the HAUP (this polarimeter is described by Dijkstra *et al* 1991). They were not clamped, because any stress could induce additional birefringence effects. For thermal isolation the barrel that contained the sample and the polarizers was exhausted. This implies that the optical properties we measured are those for zero pressure. A diaphragm was mounted between the first polarizer and the sample. The sample could be oriented perpendicular to the light beam by directing the beams that were reflected from both surfaces of the sample back through the diaphragm. This could be done with an accuracy of approximately 0.5 mm, which corresponds to an angle of 8.3×10^{-3} rad $= 0.5°$ (distance of diaphragm from sample surface: 6 cm). The wavelength used was $\lambda_0 = 632.8$ nm, except in the case of sample S_5 where 543 nm was used.

The six samples measured will be referred to as S_i with $i = 1, \ldots, 6$. The normals to the surfaces are given on a cartesian basis $\{\hat{x}, \hat{y}, \hat{z}\}$, with $\hat{x} \parallel a$, $\hat{y} \parallel b$ and

$\hat{z} \parallel c$ and the thicknesses

Sample		Orientation	Thickness
S_1	:	$\hat{x}$	$d = 2.57 \pm 0.02$ mm
S_2	:	$\hat{y}$	$d = 2.485 \pm 0.003$ mm
S_3	:	$\hat{z}$	$d = 2.57 \pm 0.02$ mm
S_4	:	$\hat{y} + \hat{z}$	$d = 1.95 \pm 0.02$ mm
S_5	:	$\cos(53°)\hat{x} + \sin(53°)\hat{z}$	$d = 2.45 \pm 0.02$ mm
S_6	:	$\hat{x} + \hat{y}$	$d = 1.45 \pm 0.02$ mm. (2)

4. Birefringence

With an Abbe refractometer and also by the method of the minimum deviation angle (see e.g. Wahlstrom 1979) we determined the mean refractive index

$$\bar{n} = 1.527 \pm 0.002. \tag{3}$$

A polarizing microscope with a Berek compensator were used to determine the signs of the birefringences. The birefringences $\Delta n(100) = n_c - n_b$ and $\Delta n(001) = n_a - n_b$ for waves propagating along the a and the c direction, respectively, are positive for wavelengths between 400 nm and 650 nm (room temperature and 1 atm pressure). The birefringence $\Delta n(010) = n_a - n_c$ for waves propagating along the b-direction is negative for 650 nm and positive for 500 nm and 400 nm (room temperature and 1 atm pressure). From the HAUP data on the birefringence (figures 1 to 6) we can derive that for 632.8 nm and zero pressure $\Delta n(010)$ is positive. So we have for the birefringences $\Delta n(S_i)$ of the different samples S_i (defined so that they are all positive at room temperature)

$$
\begin{aligned}
\Delta n(S_1) &= \Delta n(11) = n_c - n_b &&= \Delta n(100) \\
\Delta n(S_2) &= \Delta n(22) = n_a - n_c &&= \Delta n(010) \\
\Delta n(S_3) &= \Delta n(33) = n_a - n_b &&= \Delta n(001) \\
\Delta n(S_4) &= \Delta n(23) = n_a - 0.50(n_c + n_b) &&= 0.50\Delta n(001) + 0.50\Delta n(010) \\
\Delta n(S_5) &= \Delta n(13) = 0.64n_a + 0.36n_c - n_b &&= 0.64\Delta n(001) + 0.36\Delta n(100) \\
\Delta n(S_6) &= \Delta n(12) = n_c - 0.50(n_a + n_b) &&= 0.50\Delta n(100) - 0.50\Delta n(010)
\end{aligned}
\tag{4}
$$

where the convention adopted for $\Delta n(ij)$ is the same as the one used for the gyration coefficient (see (5)) and where we have used in the last three expressions that $\Delta n(100)$, $\Delta n(010)$ and $\Delta n(001)$ are small with respect to n_a, n_b and n_c. We can see that with these definitions for the birefringences $\Delta n(001) = \Delta n(100) + \Delta n(010)$, and indeed this can be observed also in the figures 1, 2 and 3.

In figures 1 to 6 we see that all the birefringences (accidentally) go through zero in the INC phase; this happens for different directions at slightly different temperatures, so there is no temperature at which TMAZC becomes optically isotropic. For all samples we could detect T_i and T_c in the birefringence (although not visible in
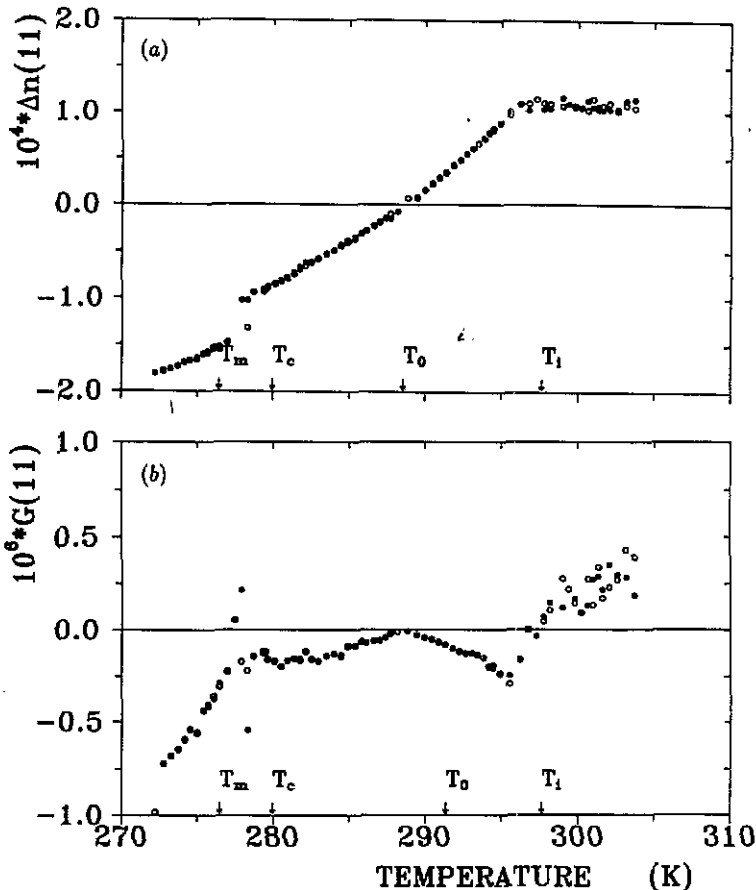
Figure 1. The birefringence $\Delta n(11) = \Delta n(100)$ (*a*) and the optical activity $G(11) = g_{11}$ (*b*) in phases I, II, III and IV of TMAZC. Open circles refer to measurements with the incident light polarized along *c*, full circles to those with the light polarized along *b*. Note that most of the data for both polarizations is equal and that, for these data the open circles are not visible.

figure 3 for S_3). We see that the modulation affects the birefringences significantly. The results are in agreement with those of Saito *et al* (1987). There is only one difference: in our sample we did not find $\Delta n(010)$ to change sign in the INC phase. This could be due to the use of a different light source (not mentioned by the authors). The previous attempts to measure the birefringence $\Delta n(100)$ of TMAZC by Régis *et al* (1982) and the results for $\Delta n(100)$, $\Delta n(010)$ and $\Delta n(001)$ around T_o by Vlokh *et al* (1987) are confirmed by our results. We refer to the work of Régis *et al* (1982) and Vlokh *et al* (1987) for the explanation of the temperature dependence of the birefringence.

5. Absorbance and linear dichroism

With an UV/VIS spectrophotometer the absorbance $A = (2\pi d/\lambda)\kappa$, with κ the extinction coefficient (i.e. the imaginary part of the complex refractive index), was measured for a plane-parallel sample with faces perpendicular to a and thickness
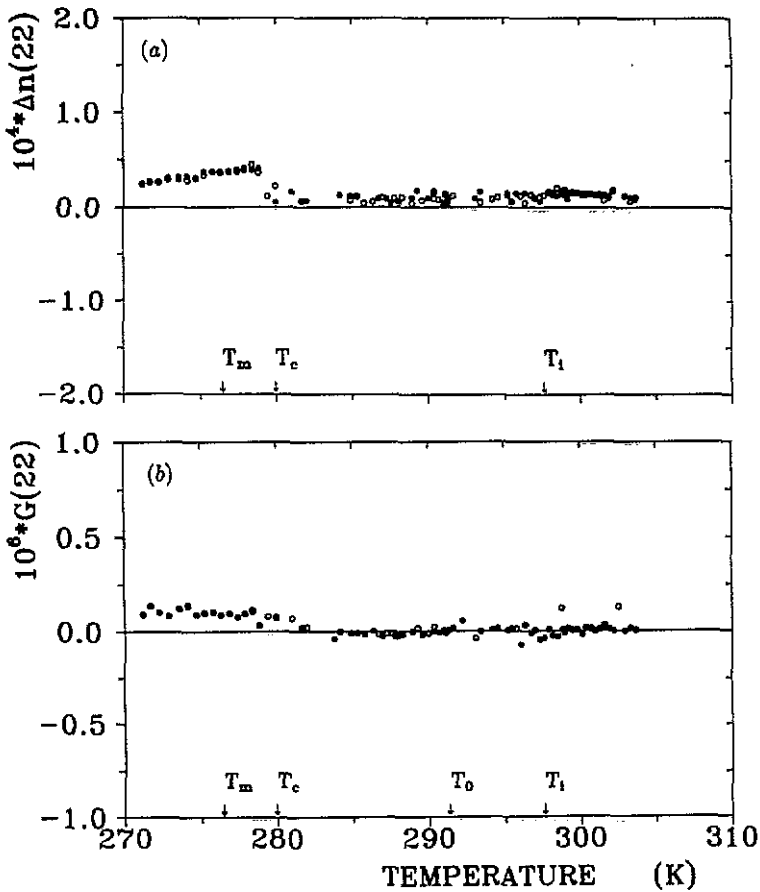
Figure 2. The birefringence $\Delta n(22) = \Delta n(010)$ (*a*) and the optical activity $G(22) = g_{22}$ (*b*) in phases I, II, III and IV of TMAZC. Open circles refer to measurements with the incident light polarized along *c*, full circles to those with the light polarized along *a*.

$d = 1.75\pm0.02$ mm (figure 7). This absorbance is obtained for unpolarized light; if we use polarized light we see that the humps at 560 nm and 890 nm only appear for light polarized along *c* and the dips at these wavelengths occur only for light polarized along *b* (in figure 7). For all the presented experiments on the optical properties a red He–Ne laser ($\lambda = 632.8$ nm) was used except for S_5, where we used a green He–Ne laser ($\lambda = 543$ nm). So we have to realize that the S_5 experiment can be influenced by the resonance at 560 nm, the other experiments are far enough away from it.

With HAUP we determined the linear dichroism for all six samples. Linear dichroism is the difference $\Delta\kappa$ between the extinction coefficients for the two eigenpolarizations. From these experiments we concluded that these can be considered to be zero within the experimental error, except perhaps for S_5. The linear dichroism of S_5 scatters a lot more than that of the other samples (but still around zero). This is caused, most probably, by the fact that only for this sample the optical properties were measured in the neighbourhood of a resonance. The results for the birefringence and optical activity are not noticeably affected.
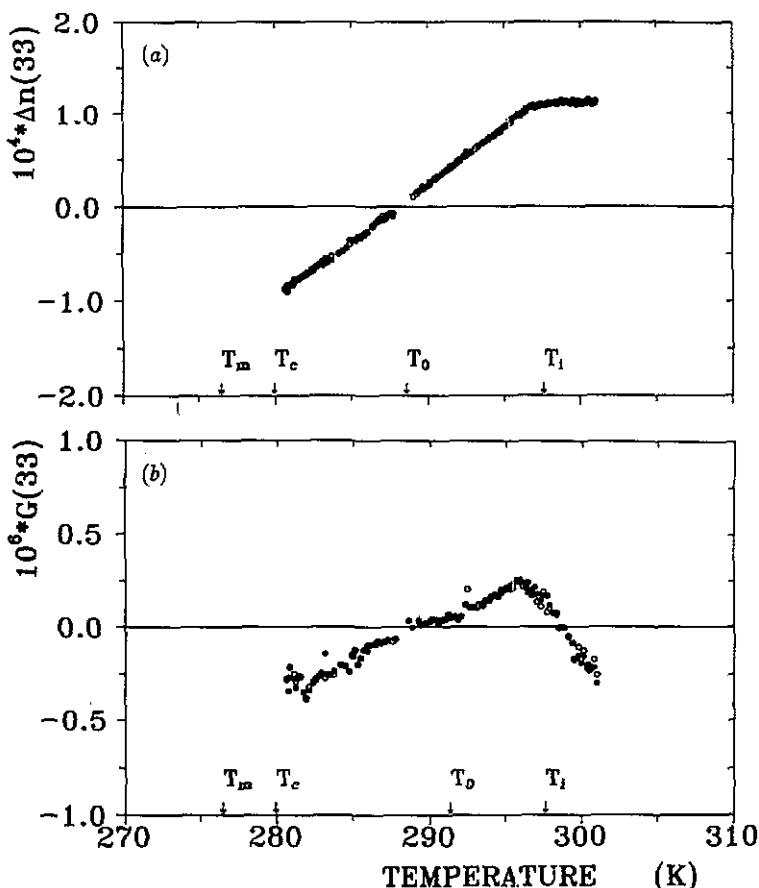
Figure 3. The birefringence $\Delta n(33) = \Delta n(001)$ (*a*) and the optical activity $G(33) = g_{33}$ (*b*) in phases I and II of TMAZC. Open circles refer to measurements with the incident light polarized along *a*, full circles to those with the light polarized along *b*.

6. Optical activity

From the HAUP data we obtained the optical activity by the fitting procedure of Moxon and Renshaw (1990) and including the so-called δY-error, which describes the deviation of the analyser orientation with respect to the polarizer due to the eccentricities of the rotation stages of both. This is explicitly described by Dijkstra *et al* (1991). The results are plotted in figures 1 to 6. The optical activities $G(S_i)$ are given by the following expressions

$$G(S_1) = G(11) = g_{11}$$
$$G(S_2) = G(22) = g_{22}$$
$$G(S_3) = G(33) = g_{33}$$
$$G(S_4) = G(23) = 0.50g_{22} + 0.50g_{33} + 1.00g_{23}$$
$$G(S_5) = G(13) = 0.36g_{11} + 0.64g_{33} + 0.96g_{13}$$
$$G(S_6) = G(12) = 0.50g_{11} + 0.50g_{22} + 1.00g_{12}.$$

(5)

We have to note that measurements on other samples with different thicknesses always gave qualitatively comparable results. Also the signs obtained for $G(ij)$ were
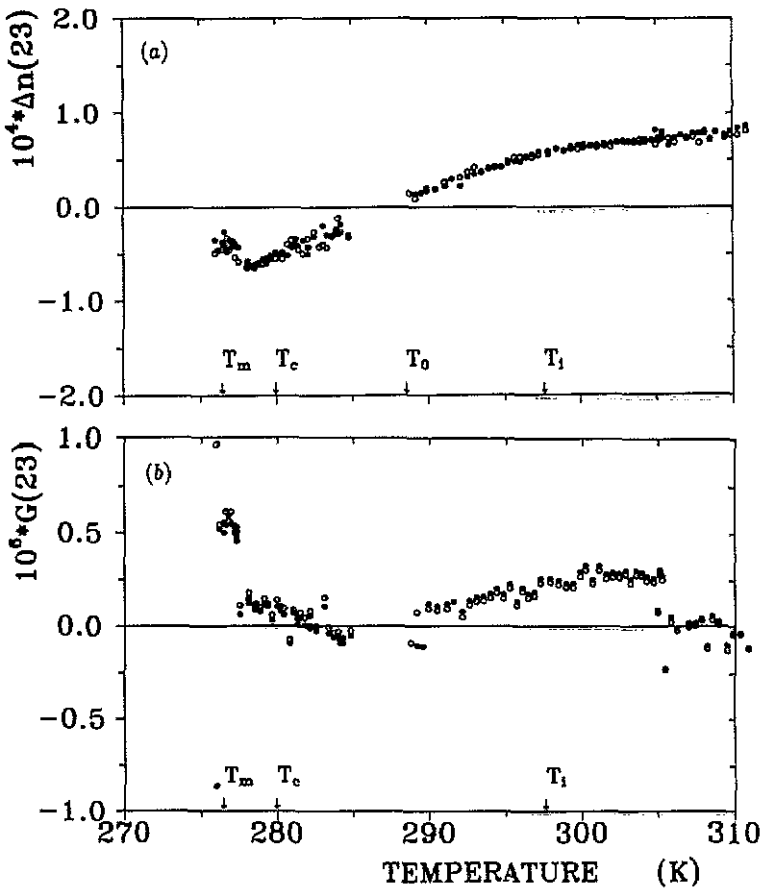
Figure 4. The birefringence $\Delta n(23) = 0.50\Delta n(001) + 0.50\Delta n(010)$ (*a*) and the optical activity $G(23) = (0.50g_{22} + 0.50g_{33} + 1.00g_{23})$ (*b*) in phases I, II and III of TMAZC. Open circles refer to measurements with the incident light polarized perpendicularly to *a*, closed circles to those with the light polarized along *a*.

the same for all these samples. Negative G indicates dextrorotatory power (rotating the plane of polarization clockwise for light coming towards the observer, convention of Glazer and Stadnicka 1986) and positive G indicates laevorotatory power (rotating the polarization direction counter-clockwise). The structural meaning of the signs found still has to be elucidated and to be completely sure about the dependence of the optical activity on sample and thickness, more measurements will be done.

There are some differences in the results presented here and previously published work by Kobayashi *et al* (1988), Dijkstra and Janner (1990) and Dijkstra (1991). The reason for this originates from a more refined interpretation of the data as explained by Dijkstra *et al* (1991). This new fitting procedure, introduced by Moxon and Renshaw (1990) discriminates explicitly between the optical properties of the sample and the systematic errors in the HAUP equipment. In the previous work the data were interpreted along the lines of Kobayashi *et al* (1986) for which one had to assume that in phase I of TMAZC the optical activity is zero. The fact that the new results give a different behaviour with temperature of the optical activity does not imply that HAUP is inadequate for determining this small effect, because in the data
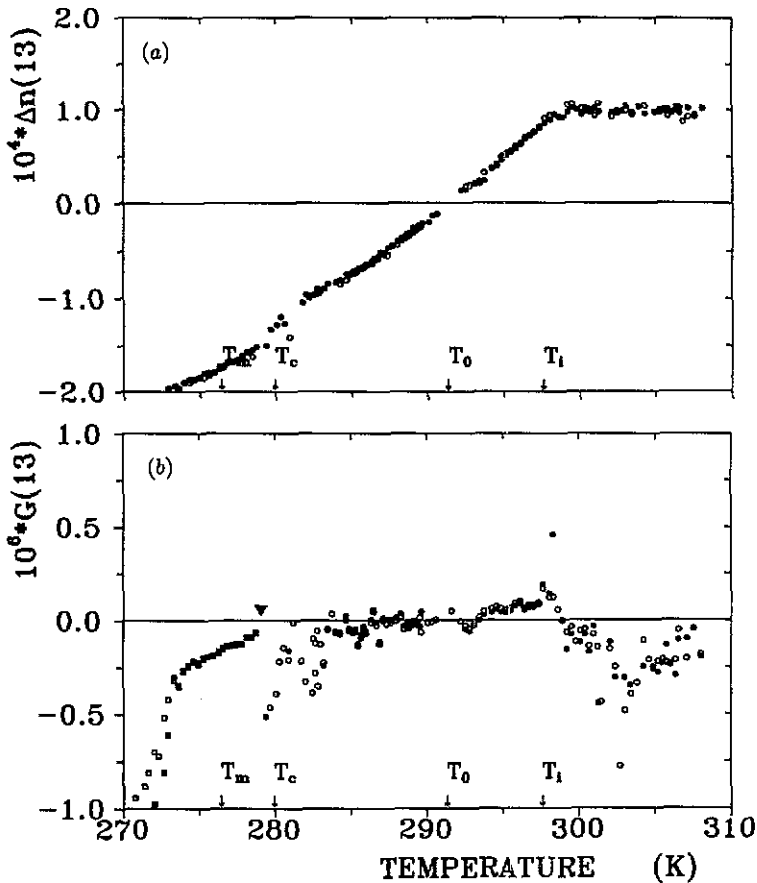
Figure 5. The birefringence $\Delta n(13) = 0.64\Delta n(001) + 0.36\Delta n(100)$ (*a*) and the optical activity $G(13) = (0.36g_{11} + 0.64g_{33} + 0.96g_{13})$ (*b*) in phases I, II, III and IV of TMAZC. Open circles refer to measurements with the incident light polarized along *b*, full circles to those with the light polarized perpendicularly to *b*. In the lock-in phase (III) and in the monoclinic phase (IV) the data on the optical activity are divided by 25 (left from ▼) in order to be able to plot these data on the same scale.

of all the presented work there is a temperature dependence that can be explained only by optical activity and not by an experimental error of the set-up.

In figure 2 we see that $G(22)$ is equal to zero in the high-temperature phase and in the INC phase. Below T_c it is slightly deviating from zero. For the other samples the optical activity is not zero in all the phases measured. Furthermore, we note that $G(13)$ becomes relatively large in the lock-in phase ($G(13) \approx 0.5 \times 10^{-5}$) and in the monoclinic phase ($G(13) > 10^{-5}$). For an interpretation of these results we refer to Dijkstra *et al* (1992).

7. Discussion

In table 1 we find the space group $Pc2_1n$ in the lock-in phase (III). Therefore the point group is $m2m$, which allows g_{13} to be different from zero (see Nye 1985). This explains $G(13)$ in this phase. In the monoclinic phase (IV) something very peculiar
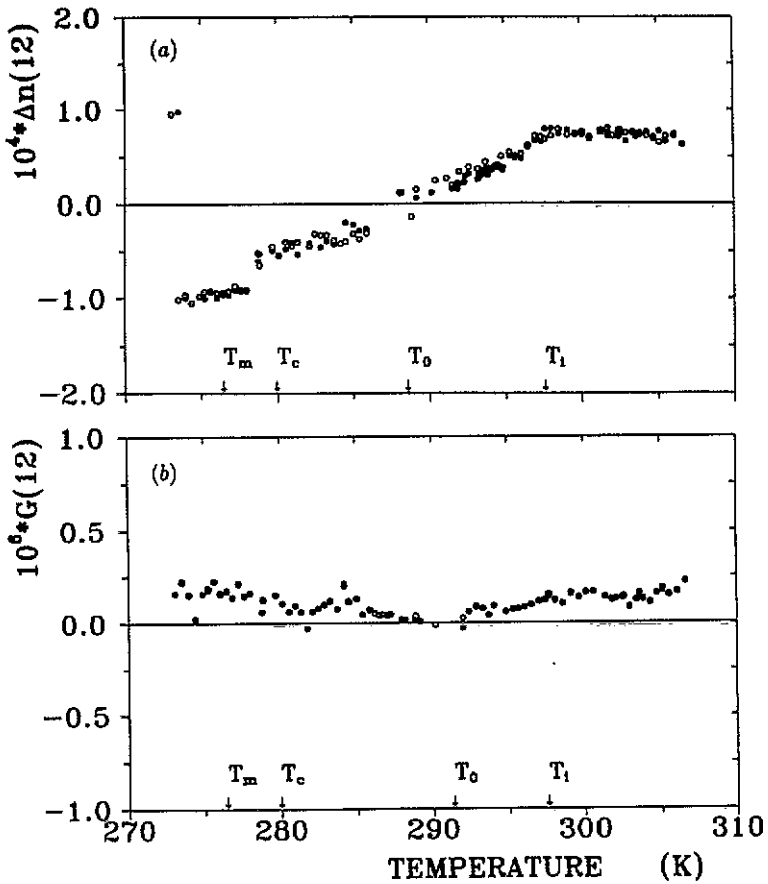
Figure 6. The birefringence $\Delta n(12) = 0.50\Delta n(100) - 0.50\Delta n(010)$ (a) and the optical activity $G(12) = (0.50g_{11} + 0.50g_{22} + 1.00g_{12})$ (b) in phases I, II, III and IV of TMAZC. Open circles refer to measurements with the incident light polarized along c, full circles to those with the light polarized perpendicularly to c.
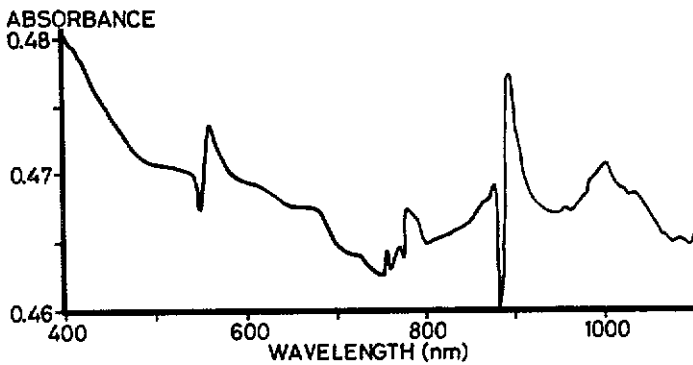

Figure 7. The absorbance of unpolarized light waves propagating along a through a TMAZC specimen of thickness $d = 1.75\pm0.02$ mm.
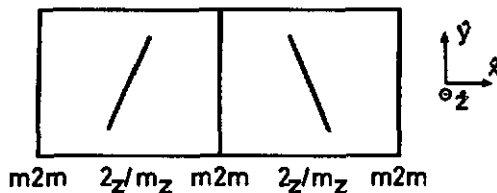
Figure 8. Schematic illustration of how the monoclinic domains ($2_z/m_z$) are seperated by domain walls with point symmetry $m2m$. Two domains are plotted, the thick lines represent one of the main axes of the dielectric tensor at different places.

causes $G(13)$ to be non-zero. From table 1 we derive that the point group ($2/m$) has inversion symmetry, and therefore no optical activity should be observed. But, the crystal on cooling down from the orthorhombic phase III to the monoclinic phase IV will consist, in general, of monoclinic domains seperated by (b, c) domain walls (Meekes *et al* 1988). This situation is schematically plotted in figure 8. The dielectric properties of such a configuration must be described by a spatial dependent dielectric tensor. Dijkstra *et al* (1992) showed that the optical properties for a periodic dielectric medium are then restricted by the point symmetry of the boundary surfaces. Here the point symmetry of the domain walls is $m2m$, for which g_{13} can be non-zero. So, this explains $G(13)$ in the monoclinic phase also. In the other samples measured we also found optical activity in the monoclinic phase, but in comparison with g_{13} the values are negligible.

In the INC phase we find for $G(11)$, $G(22)$ and $G(33)$ that g_{11} and g_{33} are unequal to zero and that g_{22} is equal to zero. This can be explained by the mesoscopic theory of optical properties in the INC phase of Dijkstra *et al* (199) to be the result of a mesoscopic periodic variation in the (a, b) plane and periodic along c of the dielectric tensor with its symmetry described by the subperiodic group $P_z ccm$.

The optical activities $G(23)$, $G(13)$ and $G(12)$ are non-zero in the INC phase, most probably due to the contributions of g_{11} and g_{33}. We cannot simply subtract these two contributions, because it is our experience that the optical activities measured in this phase are sample-dependent and it is not possible to measure more than one direction in one sample. Only global trends can be derived by comparison of the figures 1 and 3 with 4, 5 and 6. So we see for instance that in $G(13)$ for a large temperature interval in the INC phase the contributions of g_{11} and g_{33} almost cancel each other. Regarding these considerations we can only say that the contributions of g_{23}, g_{13} and g_{12} are small.

In the high-temperature phase (I) some components of the gyration tensor are different from zero, although this phase is centrosymmetric and not modulated. The reason for this, in our view, lies in the fluctuations of the mode that softens near the phase transition at T_i. The structural phase transition at T_i is the result of an instability of one of the vibrational modes of the crystal. On approaching T_i in phase I the frequency of the relevant phonon mode decreases to zero until it finally becomes a static distortion which determines the structure in the INC phase. So we can understand the optical activities measured above T_i to reflect precursive effects due to this instability.

8. Summary

The birefringence and the optical activity of TMAZC were measured in phases I, II, III and IV for six samples with different orientations. The birefringences reflect the different phase transitions. The optical activity components can be understood with the mesoscopic description of Dijkstra *et al* (1992). This theory is not only applicable to the INC phase of TMAZC but also to its multidomain monoclinic phase (IV). The optical activity measured in the INC phase is, most probably, caused by a mesoscopic periodic variation of the dielectric function together with the condition that the (001) boundaries in the crystal have point symmetry 222 (Dijkstra *et al* 1992). In the INC phase, the size of the effect is slightly sample dependent, but not depending on the thickness of the sample. The rotatory power is therefore linear with the thickness.

To come to a better verification of the mesoscopic description more measurements have to be made on TMAZC and on other materials, and also the dependence on the wavelength of the light has to be investigated.

Acknowledgments

References

Arend H, Perret R, Wüest H and Kerkoc P 1986 *J. Cryst. Growth* **74** 321
Cummins H Z 1990 *Phys. Rep.* **185** 211
Dijkstra E 1991 *J. Phys.: Condens. Matter* **3** 141
Dijkstra E and Janner A 1990 *Ferroelectrics* **105** 113
Dijkstra E, Janner A and Meekes H 1992 *J. Phys.: Condens. Matter* **4** 693
Dijkstra E, Meekes H and Kremers M 1991 *J. Phys. D: Appl. Phys.* **24** 1861
Glazer A M and Stadnicka K 1986 *J. Appl. Cryst.* **19** 108
Hogervorst A C M 1986 *PhD Thesis* Technical University Delft, The Netherlands
Iizumi M, Axe J D, Shirane G and Shimaoka K 1977 *Phys. Rev.* B **15** 4392
Kobayashi J, Kumomi H and Saito K 1986 *J. Appl. Cryst.* **19** 377
Kobayashi J, Saito K, Fukase H and Matsuda K 1988 *Phase Transitions* **12** 225
Kobayashi J and Uesu Y 1983 *J. Appl. Cryst.* **16** 204
Kobayashi J, Uesu Y, Yamada Y and Takehara H 1981 *Ferroelectrics* **36** 371
Madariaga G, Zúñiga F J, Pérez-Mato J M and Tello M J 1987 *Acta Crystallogr.* B **43** 356
Meekes H and Janner A 1988 *Phys. Rev.* B **38** 8075
Meekes H, Janner A and Janssen T 1988 *Z. Phys.* B **71** 273
Moxon J R L and Renshaw A R 1990 *J. Phys.: Condens. Matter* **2** 6807
Nye J F 1985 *Physical properties of crystals* (Oxford: Oxford University Press) ch 14
Régis M, Ribet J L and Jamet J P 1982 *J. Physique Lett.* **43** L-333
Saito K, Kawabe T and Kobayashi J 1987 *Ferroelectrics* **75** 153
Uesu Y and Kobayashi J 1985 *Ferroelectrics* **64** 115
Vlokh O G, Kityk A V and Polovinko I I 1987 *Opt. Spectrosc.* **62** 134
Wahlstrom E 1979 *Optical Crystallography* (New York: Wiley)
Wolff P M de 1972 *Acta Crystallogr.* A **28** S111